Published in final edited form as:
Neurobiol Aging. 2013 July ; 34(7): 1873–1881. doi:10.1016/j.neurobiolaging.2013.01.015.

Age-dependent regional changes in the rostral migratory stream

Arie Mobley[1], **Alex K. Bryant**[1], **Marion B. Richard**[4,5], **Jessica H. Brann**[3], **Stuart J. Firestein**[3], and **Charles A. Greer**[1,2]

[1]Department of Neurosurgery, Yale University School of Medicine, New Haven, CT 06520

[2]Department of Neurobiology,Yale University School of Medicine, New Haven, CT 06520

[3]Department of Biological Sciences, Columbia University, New York, NY

[4]INSERM U1028, CNRS UMR5292, Lyon Neuroscience Research Center, Neuroplasticity and Neuropathology of Olfactory Perception Team, Lyon, F-69000, France

[5]University of Lyon, F-69000, France

Abstract

Throughout life the subventricular zone (SVZ) is a source of new olfactory bulb (OB) interneurons. From the SVZ, neuroblasts migrate tangentially through the rostral migratory stream (RMS), a restricted route ~5 mm long in mice, reaching the OB within 10-14 days. Within the OB neuroblasts migrate radially to the granule and glomerular layers where they differentiate into granule and periglomerular (PG) cells and integrate into existing synaptic circuits. SVZ neurogenesis decreases with age, and may be a factor in age-related olfactory deficits. However, the effect of aging on the RMS and on the differentiation of interneuron subpopulations remains poorly understood. Here, we examine RMS cytoarchitecture, neuroblast proliferation and clearance from the RMS, and PG cell subpopulations in 6, 12, 18 and 23 months of age. We find that aging affects the area occupied by newly generated cells within the RMS and regional proliferation, while the clearance of neuroblasts from the RMS and PG cell subpopulations and distribution remain stable.

Keywords

Aging; Subventricular Zone; Rostral Migratory Stream; Proliferation; Migration; BrdU; Periglomerular Cells

1. Introduction

Neurogenesis occurs in the mouse subventricular zone (SVZ) throughout life and is a source of new interneurons in the olfactory bulb (OB) [11,32,33,68]. Neuroblasts migrate tangentially to the OB via the rostral migratory stream (RMS), a restricted route that is approximately 5 mm in length in mice [34,66]. During migration neuroblasts retain the

Address correspondence to: Charles A. Greer, Ph.D. Department of Neurosurgery Yale University School of Medicine P.O. Box 208082 New Haven, CT 06520-8082 203.785.4034; fax, 203-737-2159 charles.greer@yale.edu.

Disclosure statement: the authors have no conflict of interest.

ability to divide but have a longer cell cycle than proliferative cells in the SVZ (17.3 vs 12.5-14 hr), while maintaining an average migration rate of 23 μm/h [39,44,48,53,59].

The outer border of the RMS is defined by astrocytes that give the RMS the appearance of a tube-like structure [35,66]. The vasculature is pervasive within the astrocytic tube, and longitudinally oriented in parallel with the migrating neuroblasts [66]. Together, the RMS vasculature and astrocytic scaffolding form a permissive environment for neuroblast migration [6,16,66,68]. The RMS can be divided into three distinct anatomical regions (Fig. 1A): 1) The vertical arm (VA) extends from the SVZ and includes the descending region underlying the white matter of the corpus callosum; 2) The elbow is composed of the rostral curve towards the OB at the base of the VA; and 3) The horizontal arm (HA) is the final rostral extension into the OB [10].

Neuroblasts from the SVZ reach the OB 10-14 days following cell division, where they migrate radially to the OB granule and glomerular layers, differentiate, and become integrated into synaptic circuits [8,26,69]. Activity-dependent processes can modulate survival of newly arrived cells, but under normal housing conditions ~50% are integrated into the OB circuitry and the remaining are lost [31,40,49,62]. Most of the surviving neurons differentiate into granule cells, although ~5% become periglomerular (PG) cells [31].

With only a few exceptions, the most numerous interneurons found in the OB, granule cells are a molecularly homogeneous population [23,60]. However, PG cells, which surround the OB glomeruli, are a heterogeneous population of interneurons. PG cells are categorized molecularly by neurotransmitter type (dopaminergic or GABAergic) and the expression of calcium binding proteins including parvalbumin, calbindin and calretinin [28,29,67]. PG cells receive synapses from olfactory sensory neuron axons, establish reciprocal dendrodendritic synapses with mitral and tufted cells, and send axons to neighboring glomeruli [3,25,27]. PG cells thus modulate both intra- and inter-glomerular circuits and affect patterns of odorant-induced activity [19,57].

With age, deficits have been reported in olfactory discrimination and sensitivity that may reflect a decline in SVZ neurogenesis [12,14,41,52,54,64]. Experimentally induced reduction of adult neurogenesis results in a loss of innate olfactory responses as well as a diminished ability to learn olfactory related tasks [47,56,65]. Age-related decreases in SVZ neurogenesis may be due in part to a decrease in the number of dividing cells as well as diminished expression of growth factors or their signaling pathways [14,24,43,58,64].

Here, we assessed age-dependent changes in the organization of the RMS and the effects of age-related decreases in neurogenesis on subpopulations of PG cells. Cell division continues within the RMS but is affected by age in a regional manner. We have established that neuroblast migration capability is unaffected by age, although there is a decrease in the area of the RMS occupied by migrating neuroblasts resulting from a decrease in neurogenesis. Despite the age-related decline in neurogenesis, the number and distribution of PG cells remains stable.

2. Materials and methods

2.1 Animals and BrdU administration

C57 mice (National Institute on Aging – CRL) from each age group (6 months (mo), n = 8; 12 mo, n = 8; 18 mo, n = 8; 23 mo, n = 8) received 2 intraperitoneal injections of 5-bromo-2′-deoxyuridine (BrdU, 50 mg/kg) 2 hrs apart. Mice were euthanized 2 hr or 14 d (for the RMS study) or 28 d (for the PG cell study) after BrdU injection. Mice were anesthetized with pentobarbital and perfused transcardially with 0.1 M phosphate buffer

saline (PBS) with 1 unit/mL heparin, followed by 4% paraformaldehyde (PFA). Brains were post-fixed in 4% PFA for 2 hr following dissection, rinsed in PBS overnight, cryoprotected in 30% sucrose in PBS, transferred to OCT and rapidly frozen in a slurry of dry ice and ethanol and stored at −80° C until used.

2.2 Immunohistochemistry

Brains were sectioned on a cryostat into 20μm coronal sections and mounted on Superfrost Plus slides, or 50μm free floating sagittal sections were collected in 48 well tissue culture plates (Becton Dickinson Labware, NJ) in anti-freeze solution (30% sucrose, 30% ethylene glycol, 1% polyvinyl pirrolidone in 0.1 M phosphate buffer) and stored at −20 °C. Slides of coronal sections were dried in a 37°C oven for 15 min. All sections were incubated in 0.025 M HCl at 65 °C for 30 min, 0.1M borate buffer for 10 min and then PBS for 5 min. For PG cell immunostaining, sections were incubated in TBS-0.3% Triton X-100 (TBS-T) for 15 min and blocked for 1 hr in TBS-T with 3% bovine serum albumin (BSA) and 5% normal donkey serum (NDS; cat. #017-000-121; Jackson ImmunoResearch, West Grove, PA). For RMS immunostaining, free floating sections were blocked for 30 min in 3% BSA PBS-T.

Incubation with primary antibody in PBS-T (free floating) or TBS-T (slides) with 3% BSA and 5% NDS was overnight at 4 °C with the following primary antibodies: mouse monoclonal anti-BrdU (cat. #346580, 1:200; Becton Dickinson, San Jose, CA); rabbit polyclonal anti-Ki67 (cat. # NB110-89719SS, 1:1000; Novus Biologicals, Littleton, CO); rabbit polyclonal anti-tyrosine hydroxylase (TH; cat. #AB152, 1:2000; Millipore, Temecula, CA); rabbit polyclonal anti-calbindin D28K (CB; cat. #AB1778, 1:1000; Millipore); mouse monoclonal anti-calretinin (CR; cat. #MAB1568, 1:800; Millipore); mouse monoclonal anti-neuronal nuclei (NeuN; cat. #MAB377, 1:700; Millipore); goat anti-doublecortin (DCX; cat. #sc-8066, 1:500; Santa Cruz Biotechnology, Inc, Santa Cruz, CA); rat anti-platelet endothelial cell adhesion molecule (PECAM; cat. # 553370, 1:50; BD Pharmingen, San Diego, CA); rabbit anti-GFAP (cat. # M0761, 1:1000; DAKO, Carpinteria, CA); rabbit anti-cleaved caspase-3 (cat. #9661, 1:100; Cell Signaling Technology, Danvers, MA). Secondary antibodies were applied for 1 hr at room temperature in 3% BSA PBS-T or TBS-T (cat. #A21121, A21124, A21240, A31573, A31573; 1:1000; Invitrogen, Eugene, OR) with the nuclear marker DRAQ5 (cat. # DR71000, 1:1000; Biostatus Limited, Leicestershire, UK) or DAPI (cat. #D1306, 1:500; Invitrogen). For double labeling with two mouse primary antibodies, slides were fixed with 2% PFA in PBS for 15 min following the first primary and secondary antibody staining. The second primary and secondary antibodies were then applied as described. Lipofuscin fluorescence was reduced by staining with 1% Sudan Black in 70% ethanol for 1 min, clearing in 70% ethanol, and rinsing with PBS or TBS-T. Slides were coverslipped using Fluoro-Gel with Tris Buffer (cat. #17985-10; EMS, Hatfield, PA).

2.3 Image acquisition and analysis

Confocal images were captured on a Leica DMRXE microscope as either z-stacks with a 1μm step between optical sections or single plane images. Images of DCX and cleaved caspase 3 labeling were captured on an Olympus BX52-epi-fluorescent microscope from coronal sections of each RMS region (n = 3 images/region/animal, n = 3 animals/age group). Sagittal sections of the SVZ and RMS were analyzed with ImageJ Cell Counter for the number of DCX, BrdU and Ki67+ cells within each region (SVZ and VA, elbow and HA of the RMS (n = 3 images/region/animal, n = 4 animals/age group). To exclude any labeling of glia, BrdU+ cells were counted only if they were also DCX+. The length of the counted area and the elbow angle was measured in ImageJ. To analyze the average area of the RMS vasculature and glial surround, the thresholds for PECAM and GFAP images were determined by eye and the percentage of PECAM or GFAP staining within the DCX+ area was quantified (Photoshop CS2). RMS area was measured as the pixel area of DCX staining

and averaged across images from the same region (Photoshop CS2). Apoptosis was measured from cleaved caspase 3 staining as positive cell density (ImageJ). Data sets were analyzed by one-way or two-way ANOVA with Bonferroni post tests (GraphPad Prism 4). Nonparametric data were analyzed by Kruskal-Wallis test with Dunn's Multiple Comparison post test.

Analyzed images of PG immunostaining were captured on an Olympus BX51 epi-fluorescent microscope. The ventral, dorsal, medial, and lateral regions of the OB from two different rostral, middle, and caudal sections were analyzed using ImageJ Cell Counter (n = 6 images per area/animal, n = 3 animals/age group). The area of the glomerular layer (GL) was measured, and counts were obtained within the bounded GL area. Counting standards were developed for each PG cell marker that allowed consistent discrimination between positive and negative cells. Data sets were analyzed by one-way ANOVA with Bonferroni post tests.

3. Results

3.1 Cell proliferation in the SVZ and RMS

To assess age-dependent changes in SVZ cell proliferation, 6, 12, 18 and 23 month (mo) mice were injected with a non-toxic dose of BrdU (50 mg/kg) and sacrificed 2 hr later [2,13,17,64]. There was a significant age-dependent decrease in the density of BrdU+ cells in the SVZ (Fig. 1B; one-way ANOVA, $F_{3,30} = 2.878$, $p < 0.05$; Bonferroni post test 6 mo vs 23 mo, $p < 0.05$). The most precipitous drop in BrdU+ density occurred from 6 – 12 months, with a 44% reduction, after which BrdU+ cell density was relatively stable through 23 months. Since BrdU incorporation is limited to the S-phase of the cell cycle, we stained for Ki67 which labels cells throughout the cell cycle in order to sample the entire population of cycling cells. Ki67 cell density showed a similar decreasing trend with age (data not shown).

Doublecortin (DCX) staining reveals all migrating neuroblasts from the SVZ to the OB via the RMS (Fig. 1A) [15,20]. We found BrdU+/DCX+ cells throughout the length of the RMS, consistent with the notion that proliferative cells are also within the RMS. The density of BrdU+ cells throughout the RMS showed a decreasing trend with aging (Fig. 1C). A similar trend was found for Ki67 labeling (data not shown).

The division of the RMS into 3 primary regions is readily seen with DCX labeling: the VA, the elbow, and the HA (Fig.1A) [10]. In sagittal sections the VA can be clearly identified as a narrow chain of DCX+ cells running along the edge of the striatum. The elbow is defined by its bend at the ventral/rostral edge of the striatum. The HA is a wider chain of DCX+ cells that widens further as DCX+ cells disperse around the caudal OB. Proliferation may occur preferentially in a specific region of the RMS. To determine the distribution of cell division along the RMS we utilized antibodies against BrdU, Ki67 and DCX on sagittal brain sections, and then separately analyzed the three RMS regions. Our caution to limit data collection to each region resulted in an average VA length of 636.21 +/− 33.32 μm across ages. The average angle of the elbow was 134.9 +/− 1.59 degrees. The average distance analyzed towards the VA from the elbow focal point was 297.47 +/− 21.32 μm and 269.95 +/− 15.44 μm towards the HA for a total average elbow length of 567.42 +/− 30.66 μm. The average HA length measured was 322.86 +/− 34.01 μm. Within each region and across ages DCX+ neuroblasts were evident (Fig. 2A-C). We then measured the density of both BrdU+ and Ki67+ cells within the RMS delineated by DCX staining. At two hours (hrs) post-injection there is frequent colocalization between BrdU and Ki67. In the VA (Fig. 2D) BrdU + cell density decreased significantly during aging (BrdU, one-way ANOVA, F3, 44 = 3.929, $p < 0.05$; Bonferroni post test 6 mo vs 23 mo, $p < 0.05$. Ki67 labeled more cells than

BrdU in the VA and had a decreasing trend with age (data not shown). In contrast, in the elbow and HA the density for both Ki67+ (data not shown) and BrdU+ cells (Fig. 2E-F) did not differ across aging. The age-dependent decrease in cell division in the SVZ and VA suggests that the VA may be more similar to, or an extension of, the SVZ than the elbow, where proliferation decreases were not significant or the HA where uniform proliferation occurred across ages.

3.2 Cell death in the RMS

To address the possibility that the decrease in BrdU+ or Ki67+ cell density during aging was due to an increase in cell death, we used the apoptotic marker cleaved caspase 3. However, we did not find any significant differences in cleaved caspase 3 cell density across age groups, within the SVZ or in DCX-delineated regions of the RMS (data not shown, one-way ANOVA for each region, $p > 0.05$).

3.3 Cytoarchitecture of the RMS

Changes in the frequency of cell division in the SVZ and in the VA of the RMS may predict changes in the area occupied by immature migrating neuroblasts or in the architecture of the RMS. Using coronal sections we measured the area (μm^2) from each RMS region, as defined by DCX labeling (Fig. 3A-C). Both the elbow and HA showed significant decreases in the area occupied by DCX+ cells with aging, while the VA showed a decreasing trend (Fig. 3D-F). These data suggested that changes to the cytoarchitecture of the RMS might occur with age. However, when the average areas of PECAM+ and GFAP+ labeling were measured within the DCX-defined RMS, no significant differences were found across ages (PECAM: 6 mo, 9.87+/−1.09; 12 mo, 11.94+/−1.79; 18 mo, 11.68+/−1.87; 23 mo, 10.33+/−0.71: GFAP: 6 mo, 33.03+/−7.24; 12 mo, 26.10+/−1.97; 18 mo, 32.08+/−2.65; 23 mo, 25.46+/−1.68), suggesting that despite the lower number of migrating neuroblasts, the vascular and astrocytic scaffolding are preserved during aging. Thus, the age-dependent decrease in neuroblast number is not due to a decrease in cytoarchitectural support from the vasculature and astrocytes.

3.4 Migration in the RMS

Neuroblast migration in the RMS occurs in longitudinally oriented chains (eg. Fig. 2A-C) [35]. A reduction in the RMS area occupied by DCX+ neuroblasts may reflect changes in the number of neuroblasts exiting the SVZ or the capability to migrate through the RMS. To address these issues, we compared the density of BrdU+ cells in the SVZ or RMS at 2 hr and 14 d post BrdU injection in mice from each age group (Fig. 4). At 14 d post BrdU injection there is no significant difference in the density of BrdU+ cells across ages in the SVZ (Bonferroni post test 14 d, $p > 0.05$). A Kruskal-Wallis test on the percentage of reduction across ages was not significant. Two-way ANOVA revealed that the effect of age was dependent on the post injection time point (Age, $F3, 45 = 4.480$, $p < 0.01$; Time post injection, $F1, 45 = 29.800$, $p < 0.0001$; Bonferroni post test 2 hr, 6 vs 12 and 23 mo, $p < 0.001$ and 6 vs 18 mo, $p < 0.05$; Interaction, $F3, 45 = 6.620$, $p < 0.001$). Thus, although SVZ proliferation is higher at 6 mo, as seen at the 2 hr time point (as shown in Fig.1B), by 14 d post injection the density of labeled cells is equivalent across all ages. These data suggest that regardless of age, neuroblasts successfully exit the SVZ within 14 days.

Next, we examined neuroblast migration through the RMS. Two-way ANOVA found that age was not a significant factor in a comparison of BrdU+ cell density across ages between 2 hr and 14 days within the RMS ($F3, 12 = 3.13$, $p > 0.05$) and there was no significant interaction with time post injection ($F3, 12 = 1.28$, $p > 0.05$) suggesting that the capability of neuroblast migration does not change with age (Fig. 5). Only time post-injection was a significant factor ($F_{3,12} = 33.50$, $p < 0.0001$) describing the decrease of BrdU+ neuroblasts

between 2 hr and 14 days. A comparison of the percent reduction across ages was not significantly different (Kruskal-Wallis, $p > 0.05$). Collectively, these data suggest that age does not significantly affect neuroblast migration capability through the RMS.

3.5 PG cell fate and aging

We next sought to understand how a decrease in cell proliferation and neuroblast migration through the RMS into the OB translates into the composition of OB interneurons. We had previously shown that the population of PG cells as a whole was not affected by aging, but did not address the possibility that subpopulations may be differentially affected [55] The cells generated in the SVZ and RMS are fated for two different populations of interneurons in the OB, the granule cells and the PG cells [9,38,71]. The former constitutes the largest population of cells in the OB and are a predominately homogeneous population [23,60]. In contrast, although PG cells are fewer in number they consist of multiple subpopulations based on the expression of calcium binding proteins and neurotransmitters [29,67]. We first asked if PG cell subpopulations in the glomerular layer (GL) are differentially affected by aging. We labeled OB sections for NeuN, calretinin, calbindin and tyrosine hydroxylase in 6, 12, 18 and 23 mo mice (Fig. 6A-D). NeuN accounted for the majority of PG cells (Fig. 6E) [70]. The fewest cells were labeled by calbindin and tyrosine hydroxylase while calretinin labeled an intermediate number of PG cells. For each subpopulation of PG cells, there were no age-dependent differences in mean cell density (Fig. 6E). This stability across aging is confirmed when each OB region is analyzed separately (data not shown; same regions as in Fig. 7C).

We then determined the density of BrdU+ cells in the GL 28 days after BrdU injection at 6, 12, 18 and 23 mo (Fig. 7A-A”). Overall BrdU+ cell density in the GL significantly decreases during aging (Fig. 7B; one-way ANOVA, $F3, 8 = 25.59$, $p < 0.001$). More precisely, GL BrdU+ cell density is stable between 6-12 mo, decreases from 12 to 18 mo and stabilizes thereafter through 23 mo (Bonferroni post test 6 and12 vs 18 and 23 mo, $p < 0.01$). At 23 mo overall BrdU+ density is 72% lower than at 6 mo. At each age, BrdU+ cells were distributed evenly throughout the GL regions (Fig. 7C). We observed a similar pattern of BrdU+ cell density decrease with age for each anatomical region analyzed (two-way ANOVA, age, not region, is a significant factor, $p < 0.001$, Bonferroni post test compared to 6 or 12 mo, $p < 0.05$ indicated by black or red asterisk, respectively). These data suggest that newly generated cells fated for the GL of the OB distribute equally across all OB regions regardless of age, and contribute to a stability of the PG cell population.

4. Discussion

Here we present several important findings on the effect of aging on the SVZ and RMS. First we confirmed an age dependent decrease in the SVZ, and extended that research to the RMS where cell proliferation decreased with age non-uniformly within the 3 RMS regions. The change in RMS proliferation was not due to a decrease in neuroblast exit from the SVZ, neuroblast migration capability or alterations to vascular and glial cytoarchitecture, although the area of the RMS occupied by migrating neuroblasts was decreased. Finally, we measured an overall stability in PG cell subpopulations across ages, despite the reduction in newly generated PG cells with age.

4.1 Neurogenesis during aging

The decrease in cell division in the SVZ seen with both BrdU and Ki67 is consistent with earlier reports [14,54,64]. The abrupt decrease in labeling from 6 to 12 months may reflect an increase in the number of quiescent progenitor cells or an overall decrease in the number of progenitor cells [1,5,37]. From 12 to 23 months the density of proliferating cells (BrdU+

or Ki67+) in the SVZ remained relatively stable. While discussions of olfactory related neurogenesis most often focus on the SVZ, dividing precursors (i.e. neuroblasts) are also found throughout the RMS [21,53]. The short 2 hr interval between BrdU injection and sacrifice and because Ki67 labels cells within the cell cycle at the time of sacrifice, both markers strongly suggest that proliferating neuroblasts are present within the RMS and not restricted solely to the SVZ. The BrdU analyses of the RMS showed an age-dependent decline in the density of labeled cells that was more gradual compared to the SVZ. This decrease was not due to changes in neuroblast exit from the SVZ, as measured by the reduction in BrdU+ cell density in the SVZ from 2 hr to 14 days post-injection. Of further interest, the BrdU analyses of the three primary regions of the RMS established that cell division within both the elbow and HA were stable during aging, while the VA showed a significant decline over the course of 6 to 23 months. Thus, it seems reasonable to suggest that the proliferation decline noted in the RMS is largely a function of the decline in the VA (cf. Figures 1C and 2D). The data further suggest that proliferation in the RMS, beyond 6 months, occurs predominately within the elbow, with fewest labeled cells found in the HA and declining numbers found in the VA. Longer cell cycles have been reported with aging [22,64]. If the average migration rate of 23 μm/h is maintained with aging, neuroblasts with a longer cell cycle may migrate through the VA before dividing, supporting our data showing decreased proliferation in the VA and stable proliferation in the elbow and HA [39,48,59,64].

4.2 Structural integrity of the RMS during aging

We found that the area of the RMS occupied by DCX+ migrating neuroblasts decreased significantly during aging. DCX labels all migrating neuroblasts and immature neurons, regardless of birthdate [20]. Therefore, with the decrease in cell proliferation in both the SVZ and the RMS, a decrease in the area occupied by migrating DCX+ cells was predicted. Specifically, decreased proliferation in the SVZ and VA (Figs. 1B and 2D) manifests as fewer neuroblasts migrating through the elbow and HA resulting in a decreased DCX+ area (Fig. 3E-F). To pursue the cellular organization of the RMS further we used PECAM and GFAP to characterize the vasculature and glial surround in the RMS. The vasculature in the RMS is longitudinally organized, occurs at a higher density than in areas outside of the RMS and has been implicated in the dynamics of migratory cells within the RMS [6,66]. There has also been a suggestion that like the SVZ, the specialized vascular niche within the RMS may locally influence progenitor proliferation [50,63]. However, we found no differences in the average area of PECAM or GFAP labeling density suggesting that neither PECAM nor GFAP area is a factor in the proliferation changes measured by BrdU and Ki67.

4.3 RMS migration during aging

In spite of the significant decrease in proliferation, neuroblasts exited the SVZ and migrated through the RMS within 14 days regardless of age. The significant decrease in the number of BrdU+ cells in the RMS is consistent with a migration of labeled cells out of the RMS, as we established that cell death in the RMS (cleaved caspase 3 labeling) was not increased with aging.

4.4 Periglomerular cell fate

To establish the effects of a decrease in neurogenesis in the SVZ and RMS on cell populations within the OB, we examined PG cells because they are neatly divisible into subpopulations based on the expression of neurotransmitter and calcium binding proteins. We show here that the density of PG cells surviving 28 days after BrdU injection in the GL decreases significantly in an age-dependent manner, consistent with the decrease in neurogenesis in the SVZ. Of particular interest, the decline in the number of adult born PG cells is nonlinear. There is an accelerated decline in middle aged mice with negligible

changes in young adult and elderly mice, suggesting that the decreased proliferation in the SVZ between 6 and 12 mo has only a modest initial effect on new PG cells. The rostral RMS (HA) is a neurogenic niche for new PG cells [18,45]. Because we observed no significant changes in the density of proliferating cells within the HA, these data suggest a larger role for the RMS in new PG cell production. Changes in 28 days old PG cells might result from a reduction in newborn cell survival within the GL layer as previously reported for newborn granule cells [54]. In broader terms, these data are consistent with results from the accessory olfactory bulb, where a significant decrease in interneurons, originating in the SVZ, was observed with age [51]. Neurogenesis in the peripheral olfactory system also declines with age, but maintains a robust regenerative capacity to produce new neurons after insult [7,36].

We showed previously that the total number of PG cells is not affected by aging [55]. We extend these data by showing here that the density of PG cell subtypes is uniform throughout the OB with aging. Moreover, at each age all PG cell subtypes are evenly distributed in the GL. It is important to note that within a month after BrdU administration, ~50% of newly generated cells will undergo cell death while an additional ~25% fail to incorporate into synaptic circuits in the following two weeks [31,68,69]. Because we found no changes in cleaved caspase 3 density throughout aging, the long-term survival of PG cells is likely extended [61]. The arrival of newborn cells may be important for the acquisition of new odor-related behaviors [29,41,45].[30,42,46]. Consequently, the decrease in new PG cells may influence aspects of odor information processing. Further, there is a significant decrease in synaptic density specific to the GL with aging; the loss of dendrodendritic glomerular synapses between mitral/tufted cells and PG cells is greater than the loss of axodendritic synapses between olfactory sensory neuron axons and mitral/tufted cells [55]. Additional studies are required to determine whether PG cell stability and increased life length is sufficient to counteract the loss of synapses which may compromise olfactory circuitry and therefore, behavior related to odorant processing.

In summary, we have demonstrated that with age the RMS remains a supportive environment for migrating neuroblasts. These data have implications for studies undertaken to increase SVZ neurogenesis in aging or disease models. Our data suggest a correlation between decreased neurogenesis and an adaptive mechanism that increases PG cell life length [4,40,61]_ENREF_1. Further studies are needed to determine the effects from a decline in new OB interneurons on the olfactory system and relevant behaviors.

Acknowledgments

The authors thank Dolores Montoya and Christine Kaliszewski for technical assistance and Drs. Diego Rodriguez Gil and Fumiaki Imamura for advice and thoughtful discussions. This work was funded by NIH-NIDCD and NIH-NIA grants to CAG; ASM was supported by Neurobiology Training Grant NS 007224-24 and NRSA F32 DC010098-01A1.

6. References

[1]. Ahlenius H, Visan V, Kokaia M, Lindvall O, Kokaia Z. Neural stem and progenitor cells retain their potential for proliferation and differentiation into functional neurons despite lower number in aged brain. J Neurosci. 2009; 29(14):4408–19. [PubMed: 19357268]

[2]. Alvarez-Buylla A, Garcia-Verdugo JM. Neurogenesis in adult subventricular zone. J Neurosci. 2002; 22(3):629–34. [PubMed: 11826091]

[3]. Aungst JL, Heyward PM, Puche AC, Karnup SV, Hayar A, Szabo G, Shipley MT. Centre-surround inhibition among olfactory bulb glomeruli. Nature. 2003; 426(6967):623–9. [PubMed: 14668854]

[4]. Belvindrah R, Nissant A, Lledo PM. Abnormal neuronal migration changes the fate of developing neurons in the postnatal olfactory bulb. J Neurosci. 2011; 31(20):7551–62. [PubMed: 21593340]

[5]. Bouab M, Paliouras GN, Aumont A, Forest-Berard K, Fernandes KJ. Aging of the subventricular zone neural stem cell niche: evidence for quiescence-associated changes between early and mid-adulthood. Neuroscience. 2011; 173:135–49. [PubMed: 21094223]

[6]. Bozoyan L, Khlghatyan J, Saghatelyan A. Astrocytes control the development of the migration-promoting vasculature scaffold in the postnatal brain via VEGF signaling. J Neurosci. 2012; 32(5):1687–704. [PubMed: 22302810]

[7]. Brann JH, Firestein S. Regeneration of new neurons is preserved in aged vomeronasal epithelia. J Neurosci. 2010; 30(46):15686–94. [PubMed: 21084624]

[8]. Carleton A, Petreanu LT, Lansford R, Alvarez-Buylla A, Lledo PM. Becoming a new neuron in the adult olfactory bulb. Nat Neurosci. 2003; 6(5):507–18. [PubMed: 12704391]

[9]. De Marchis S, Bovetti S, Carletti B, Hsieh YC, Garzotto D, Peretto P, Fasolo A, Puche AC, Rossi F. Generation of distinct types of periglomerular olfactory bulb interneurons during development and in adult mice: implication for intrinsic properties of the subventricular zone progenitor population. J Neurosci. 2007; 27(3):657–64. [PubMed: 17234597]

[10]. De Marchis S, Fasolo A, Puche AC. Subventricular zone-derived neuronal progenitors migrate into the subcortical forebrain of postnatal mice. J Comp Neurol. 2004; 476(3):290–300. [PubMed: 15269971]

[11]. Doetsch F, Garcia-Verdugo JM, Alvarez-Buylla A. Cellular composition and three-dimensional organization of the subventricular germinal zone in the adult mammalian brain. J Neurosci. 1997; 17(13):5046–61. [PubMed: 9185542]

[12]. Doty RL, Petersen I, Mensah N, Christensen K. Genetic and environmental influences on odor identification ability in the very old. Psychol Aging. 2011; 26(4):864–71. [PubMed: 21639645]

[13]. Duque A, Rakic P. Different effects of bromodeoxyuridine and [3H]thymidine incorporation into DNA on cell proliferation, position, and fate. J Neurosci. 2011; 31(42):15205–17. [PubMed: 22016554]

[14]. Enwere E, Shingo T, Gregg C, Fujikawa H, Ohta S, Weiss S. Aging results in reduced epidermal growth factor receptor signaling, diminished olfactory neurogenesis, and deficits in fine olfactory discrimination. J Neurosci. 2004; 24(38):8354–65. [PubMed: 15385618]

[15]. Francis F, Koulakoff A, Boucher D, Chafey P, Schaar B, Vinet MC, Friocourt G, McDonnell N, Reiner O, Kahn A, McConnell SK, Berwald-Netter Y, Denoulet P, Chelly J. Doublecortin is a developmentally regulated, microtubule-associated protein expressed in migrating and differentiating neurons. Neuron. 1999; 23(2):247–56. [PubMed: 10399932]

[16]. García-Marqués J, De Carlos JA, Greer CA, Lopez-Mascaraque L. Different astroglia permissivity controls the migration of olfactory bulb interneuron precursors. Glia. 2010; 58(2): 218–30. [PubMed: 19610095]

[17]. García-Verdugo JM, Ferron S, Flames N, Collado L, Desfilis E, Font E. The proliferative ventricular zone in adult vertebrates: a comparative study using reptiles, birds, and mammals. Brain Res Bull. 2002; 57(6):765–75. [PubMed: 12031273]

[18]. Giachino C, Taylor V. Lineage analysis of quiescent regenerative stem cells in the adult brain by genetic labelling reveals spatially restricted neurogenic niches in the olfactory bulb. Eur J Neurosci. 2009; 30(1):9–24. [PubMed: 19558606]

[19]. Gire DH, Schoppa NE. Control of on/off glomerular signaling by a local GABAergic microcircuit in the olfactory bulb. J Neurosci. 2009; 29(43):13454–64. [PubMed: 19864558]

[20]. Gleeson JG, Lin PT, Flanagan LA, Walsh CA. Doublecortin is a microtubule-associated protein and is expressed widely by migrating neurons. Neuron. 1999; 23(2):257–71. [PubMed: 10399933]

[21]. Gritti A, Bonfanti L, Doetsch F, Caille I, Alvarez-Buylla A, Lim DA, Galli R, Verdugo JM, Herrera DG, Vescovi AL. Multipotent neural stem cells reside into the rostral extension and olfactory bulb of adult rodents. J Neurosci. 2002; 22(2):437–45. [PubMed: 11784788]

[22]. Hurtado-Chong A, Yusta-Boyo MJ, Vergano-Vera E, Bulfone A, de Pablo F, Vicario-Abejon C. IGF-I promotes neuronal migration and positioning in the olfactory bulb and the exit of

neuroblasts from the subventricular zone. Eur J Neurosci. 2009; 30(5):742–55. [PubMed: 19712103]

[23]. Imamura F, Nagao H, Naritsuka H, Murata Y, Taniguchi H, Mori K. A leucine-rich repeat membrane protein, 5T4, is expressed by a subtype of granule cells with dendritic arbors in specific strata of the mouse olfactory bulb. J Comp Neurol. 2006; 495(6):754–68. [PubMed: 16506198]

[24]. Jin K, Sun Y, Xie L, Batteur S, Mao XO, Smelick C, Logvinova A, Greenberg DA. Neurogenesis and aging: FGF-2 and HB-EGF restore neurogenesis in hippocampus and subventricular zone of aged mice. Aging Cell. 2003; 2(3):175–83. [PubMed: 12882410]

[25]. Kasowski HJ, Kim H, Greer CA. Compartmental organization of the olfactory bulb glomerulus. J Comp Neurol. 1999; 407(2):261–74. [PubMed: 10213094]

[26]. Kelsch W, Sim S, Lois C. Watching synaptogenesis in the adult brain. Annu Rev Neurosci. 2010; 33:131–49. [PubMed: 20572770]

[27]. Kiyokage E, Pan YZ, Shao Z, Kobayashi K, Szabo G, Yanagawa Y, Obata K, Okano H, Toida K, Puche AC, Shipley MT. Molecular identity of periglomerular and short axon cells. J Neurosci. 2010; 30(3):1185–96. [PubMed: 20089927]

[28]. Kosaka K, Aika Y, Toida K, Heizmann CW, Hunziker W, Jacobowitz DM, Nagatsu I, Streit P, Visser TJ, Kosaka T. Chemically defined neuron groups and their subpopulations in the glomerular layer of the rat main olfactory bulb. Neurosci Res. 1995; 23(1):73–88. [PubMed: 7501303]

[29]. Kosaka K, Toida K, Aika Y, Kosaka T. How simple is the organization of the olfactory glomerulus?: the heterogeneity of so-called periglomerular cells. Neurosci Res. 1998; 30(2):101–10. [PubMed: 9579643]

[30]. Lazarini F, Lledo PM. Is adult neurogenesis essential for olfaction? Trends Neurosci. 2011; 34(1):20–30. [PubMed: 20980064]

[31]. Lemasson M, Saghatelyan A, Olivo-Marin JC, Lledo PM. Neonatal and adult neurogenesis provide two distinct populations of newborn neurons to the mouse olfactory bulb. J Neurosci. 2005; 25(29):6816–25. [PubMed: 16033891]

[32]. Lledo PM, Merkle FT, Alvarez-Buylla A. Origin and function of olfactory bulb interneuron diversity. Trends Neurosci. 2008; 31(8):392–400. [PubMed: 18603310]

[33]. Lledo PM, Saghatelyan A. Integrating new neurons into the adult olfactory bulb: joining the network, life-death decisions, and the effects of sensory experience. Trends Neurosci. 2005; 28(5):248–54. [PubMed: 15866199]

[34]. Lois C, Alvarez-Buylla A. Long-distance neuronal migration in the adult mammalian brain. Science. 1994; 264(5162):1145–8. [PubMed: 8178174]

[35]. Lois C, Garcia-Verdugo JM, Alvarez-Buylla A. Chain migration of neuronal precursors. Science. 1996; 271(5251):978–81. [PubMed: 8584933]

[36]. Loo AT, Youngentob SL, Kent PF, Schwob JE. The aging olfactory epithelium: neurogenesis, response to damage, and odorant-induced activity. Int J Dev Neurosci. 1996; 14(7-8):881–900. [PubMed: 9010732]

[37]. Lugert S, Basak O, Knuckles P, Haussler U, Fabel K, Gotz M, Haas CA, Kempermann G, Taylor V, Giachino C. Quiescent and active hippocampal neural stem cells with distinct morphologies respond selectively to physiological and pathological stimuli and aging. Cell Stem Cell. 2010; 6(5):445–56. [PubMed: 20452319]

[38]. Luskin MB. Restricted proliferation and migration of postnatally generated neurons derived from the forebrain subventricular zone. Neuron. 1993; 11(1):173–89. [PubMed: 8338665]

[39]. Luskin MB, Boone MS. Rate and pattern of migration of lineally-related olfactory bulb interneurons generated postnatally in the subventricular zone of the rat. Chem Senses. 1994; 19(6):695–714. [PubMed: 7735848]

[40]. Mandairon N, Jourdan F, Didier A. Deprivation of sensory inputs to the olfactory bulb up-regulates cell death and proliferation in the subventricular zone of adult mice. Neuroscience. 2003; 119(2):507–16. [PubMed: 12770564]

[41]. Mandairon N, Peace ST, Boudadi K, Boxhorn CE, Narla VA, Suffis SD, Cleland TA. Compensatory responses to age-related decline in odor quality acuity: cholinergic

neuromodulation and olfactory enrichment. Neurobiol Aging. 2011; 32(12):2254–65. [PubMed: 20079556]

[42]. Mandairon N, Sultan S, Nouvian M, Sacquet J, Didier A. Involvement of newborn neurons in olfactory associative learning? The operant or non-operant component of the task makes all the difference. J Neurosci. 2011; 31(35):12455–60. [PubMed: 21880907]

[43]. Maslov AY, Barone TA, Plunkett RJ, Pruitt SC. Neural stem cell detection, characterization, and age-related changes in the subventricular zone of mice. J Neurosci. 2004; 24(7):1726–33. [PubMed: 14973255]

[44]. Menezes JR, Smith CM, Nelson KC, Luskin MB. The division of neuronal progenitor cells during migration in the neonatal mammalian forebrain. Mol Cell Neurosci. 1995; 6(6):496–508. [PubMed: 8742267]

[45]. Merkle FT, Mirzadeh Z, Alvarez-Buylla A. Mosaic organization of neural stem cells in the adult brain. Science. 2007; 317(5836):381–4. [PubMed: 17615304]

[46]. Moreno MM, Bath K, Kuczewski N, Sacquet J, Didier A, Mandairon N. Action of the noradrenergic system on adult-born cells is required for olfactory learning in mice. J Neurosci. 2012; 32(11):3748–58. [PubMed: 22423095]

[47]. Moreno MM, Linster C, Escanilla O, Sacquet J, Didier A, Mandairon N. Olfactory perceptual learning requires adult neurogenesis. Proc Natl Acad Sci U S A. 2009; 106(42):17980–5. [PubMed: 19815505]

[48]. Morshead CM, van der Kooy D. Postmitotic death is the fate of constitutively proliferating cells in the subependymal layer of the adult mouse brain. J Neurosci. 1992; 12(1):249–56. [PubMed: 1729437]

[49]. Mouret A, Gheusi G, Gabellec MM, de Chaumont F, Olivo-Marin JC, Lledo PM. Learning and survival of newly generated neurons: when time matters. J Neurosci. 2008; 28(45):11511–6. [PubMed: 18987187]

[50]. Nie K, Molnar Z, Szele FG. Proliferation but not migration is associated with blood vessels during development of the rostral migratory stream. Dev Neurosci. 2010; 32(3):163–72. [PubMed: 20616553]

[51]. Nunez-Parra A, Pugh V, Araneda RC. Regulation of adult neurogenesis by behavior and age in the accessory olfactory bulb. Mol Cell Neurosci. 2011; 47(4):274–85. [PubMed: 21600286]

[52]. Patel RC, Larson J. Impaired olfactory discrimination learning and decreased olfactory sensitivity in aged C57Bl/6 mice. Neurobiol Aging. 2009; 30(5):829–37. [PubMed: 17904696]

[53]. Poon A, Li Z, Wolfe GW, Lu L, Williams RW, Hayes NL, Nowakowski RS, Goldowitz D. Identification of a Chr 11 quantitative trait locus that modulates proliferation in the rostral migratory stream of the adult mouse brain. Eur J Neurosci. 2010; 32(4):523–37. [PubMed: 20718853]

[54]. Rey NL, Sacquet J, Veyrac A, Jourdan F, Didier A. Behavioral and cellular markers of olfactory aging and their response to enrichment. Neurobiol Aging. 2012; 33(3):626, e9–e23. [PubMed: 21601953]

[55]. Richard MB, Taylor SR, Greer CA. Age-induced disruption of selective olfactory bulb synaptic circuits. Proc Natl Acad Sci U S A. 2010; 107(35):15613–8. [PubMed: 20679234]

[56]. Sakamoto M, Imayoshi I, Ohtsuka T, Yamaguchi M, Mori K, Kageyama R. Continuous neurogenesis in the adult forebrain is required for innate olfactory responses. Proc Natl Acad Sci U S A. 2011; 108(20):8479–84. [PubMed: 21536899]

[57]. Schoppa NE, Urban NN. Dendritic processing within olfactory bulb circuits. Trends Neurosci. 2003; 26(9):501–6. [PubMed: 12948662]

[58]. Shook BA, Manz DH, Peters JJ, Kang S, Conover JC. Spatiotemporal Changes to the Subventricular Zone Stem Cell Pool through Aging. J Neurosci. 2012; 32(20):6947–56. [PubMed: 22593063]

[59]. Smith CM, Luskin MB. Cell cycle length of olfactory bulb neuronal progenitors in the rostral migratory stream. Dev Dyn. 1998; 213(2):220–7. [PubMed: 9786422]

[60]. Stenman J, Toresson H, Campbell K. Identification of two distinct progenitor populations in the lateral ganglionic eminence: implications for striatal and olfactory bulb neurogenesis. J Neurosci. 2003; 23(1):167–74. [PubMed: 12514213]

[61]. Sui Y, Horne MK, Stanic D. Reduced proliferation in the adult mouse subventricular zone increases survival of olfactory bulb interneurons. PLoS One. 2012; 7(2):e31549. [PubMed: 22363671]

[62]. Sultan S, Rey N, Sacquet J, Mandairon N, Didier A. Newborn neurons in the olfactory bulb selected for long-term survival through olfactory learning are prematurely suppressed when the olfactory memory is erased. J Neurosci. 2011; 31(42):14893–8. [PubMed: 22016522]

[63]. Tavazoie M, Van der Veken L, Silva-Vargas V, Louissaint M, Colonna L, Zaidi B, Garcia-Verdugo JM, Doetsch F. A specialized vascular niche for adult neural stem cells. Cell Stem Cell. 2008; 3(3):279–88. [PubMed: 18786415]

[64]. Tropepe V, Craig CG, Morshead CM, van der Kooy D. Transforming growth factor-alpha null and senescent mice show decreased neural progenitor cell proliferation in the forebrain subependyma. J Neurosci. 1997; 17(20):7850–9. [PubMed: 9315905]

[65]. Valley MT, Mullen TR, Schultz LC, Sagdullaev BT, Firestein S. Ablation of mouse adult neurogenesis alters olfactory bulb structure and olfactory fear conditioning. Front Neurosci. 2009; 3:51. [PubMed: 20582278]

[66]. Whitman MC, Fan W, Rela L, Rodriguez-Gil DJ, Greer CA. Blood vessels form a migratory scaffold in the rostral migratory stream. J Comp Neurol. 2009; 516(2):94–104. [PubMed: 19575445]

[67]. Whitman MC, Greer CA. Adult-generated neurons exhibit diverse developmental fates. Dev Neurobiol. 2007; 67(8):1079–93. [PubMed: 17565001]

[68]. Whitman MC, Greer CA. Adult neurogenesis and the olfactory system. Prog Neurobiol. 2009; 89(2):162–75. [PubMed: 19615423]

[69]. Whitman MC, Greer CA. Synaptic integration of adult-generated olfactory bulb granule cells: basal axodendritic centrifugal input precedes apical dendrodendritic local circuits. J Neurosci. 2007; 27(37):9951–61. [PubMed: 17855609]

[70]. Winner B, Cooper-Kuhn CM, Aigner R, Winkler J, Kuhn HG. Long-term survival and cell death of newly generated neurons in the adult rat olfactory bulb. Eur J Neurosci. 2002; 16(9):1681–9. [PubMed: 12431220]

[71]. Yang Z. Postnatal subventricular zone progenitors give rise not only to granular and periglomerular interneurons but also to interneurons in the external plexiform layer of the rat olfactory bulb. J Comp Neurol. 2008; 506(2):347–58. [PubMed: 18022946]

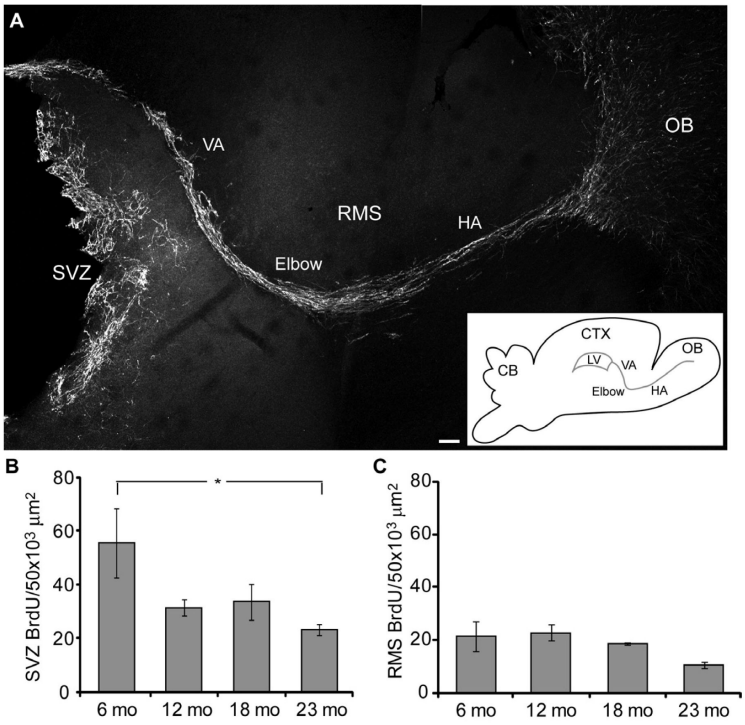

Figure 1.

Cell proliferation decreases with age in the SVZ and RMS. A, The SVZ and RMS were delineated by DCX labeling to the beginning of the OB (VA, vertical arm; HA, horizontal arm; OB, olfactory bulb). Scale bar = 100 μm. Inset, diagram of the brain, lateral ventricle (LV) and regions of the RMS (CB, cerebellum; CTX, cortex). B-C, BrdU+ cell density in the SVZ and RMS 2 hr after BrdU injection (n = 4/age group). B, SVZ, One-way ANOVA, $F_{3, 30} = 3.855$, $p < 0.05$; Bonferroni posthoc tests, 6 vs 23 mo, $p < 0.05$, indicated by asterisk. C, RMS showed a decreasing trend; One-way ANOVA, $p > 0.05$.

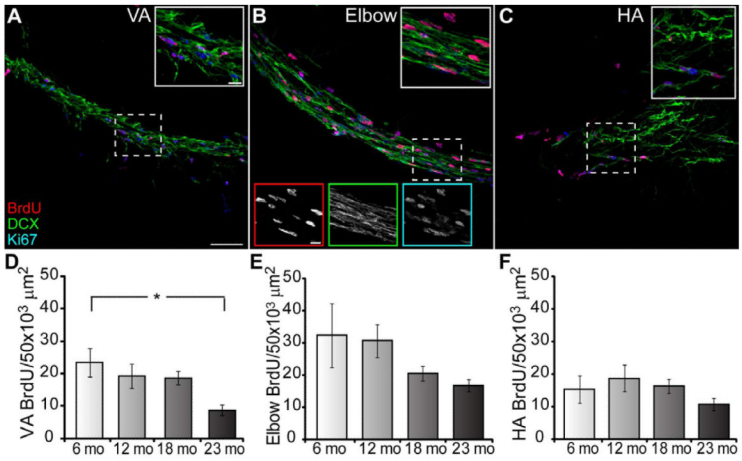

Figure 2.

Age-dependent effects on cell proliferation are region-specific within the RMS. A-C, RMS regions labeled with BrdU (red), DCX (green) and Ki67 (blue) in the VA (A), elbow (B) and HA (C); 2 hr post BrdU-injection; n = 4 animals/age group. Scale bar = 50 μm. Inset is an enlargement of the dashed box; scale bar = 50 μm. Bottom insets in B are single color images for top inset; scale bar = 20 μm. D, BrdU+ cell density in the VA significantly decreases with age (one-way ANOVA, $F_{3, 44} = 3.929$, $p < 0.05$; Bonferroni posthoc test 6 mo vs 23 mo; $p < 0.05$, indicated by asterisk). E-F, BrdU+ cell density does not significantly change with age in the elbow (E) and HA (F), although the elbow has a decreasing trend.

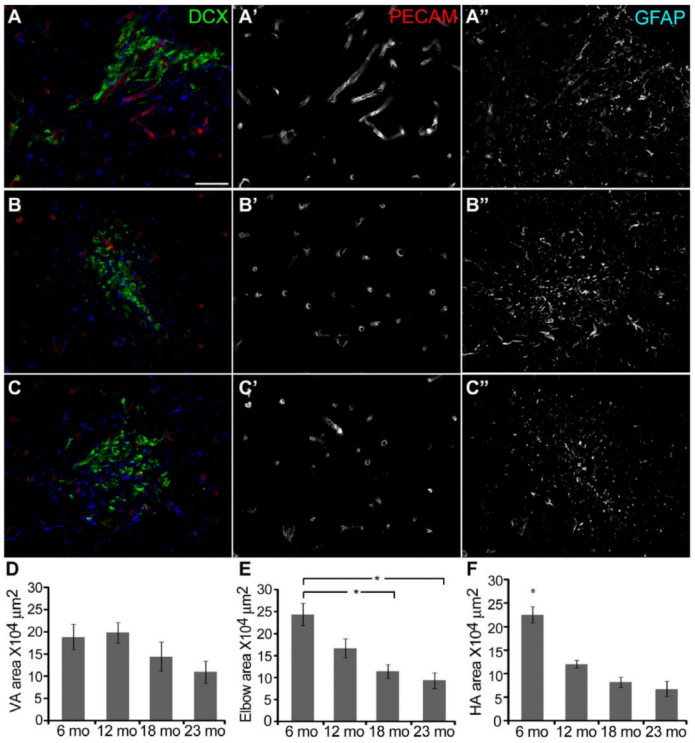

Figure 3.

The RMS area significantly decreases with age in a regional manner. A-C, Coronal sections through the VA (A), the elbow (B) and the HA (C) labeled with DCX (green), PECAM (red) and GFAP (blue). Scale bar = 20 μm. D, No age-related changes in the VA area. E, Age-related decrease in the elbow area, one-way ANOVA, $F3, 172 = 6.339$, $p < 0.0001$, Bonferroni posthoc test, 6 mo vs 18 and 23 mo, $p < 0.001$, indicated by asterisks. F, Age-related decrease in the HA area, one-way ANOVA, $F3, 173 = 3.865$, $p < 0.0001$, Bonferroni posthoc test, 6 mo vs 12, 18 and 23 mo, $p < 0.001$, indicated by asterisk.

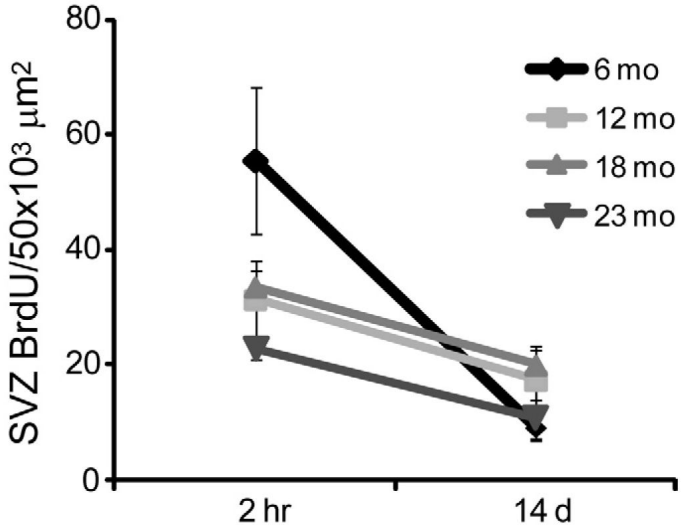

Figure 4.

The capability of neuroblasts to exit the SVZ is unaffected by age. At 14 days post-BrdU injection there is no significant difference across ages in BrdU+ cell density, suggesting that neuroblasts successfully exit the SVZ regardless of age. Results from two-way ANOVA show that only time post injection was a significant factor ($F1, 12 = 19.66$, $p < 0.001$). Age was not a significant factor and there was no significant interaction ($p > 0.05$).

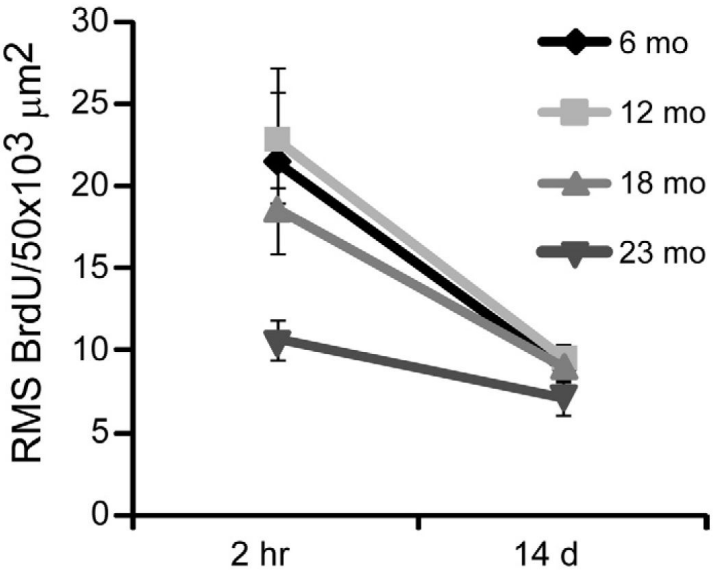

Figure 5.

Neuroblast migration capability through the RMS is unaffected by age. At 14 days post-BrdU injection there is no significant difference across ages in BrdU+ cell density, suggesting that neuroblasts successfully exit the RMS regardless of age. Results from two-way ANOVA show that only time post injection was a significant factor ($F_{1, 12} = 33.50$, $p < 0.0001$). Age was not a significant factor and there was no significant interaction $p > 0.05$).

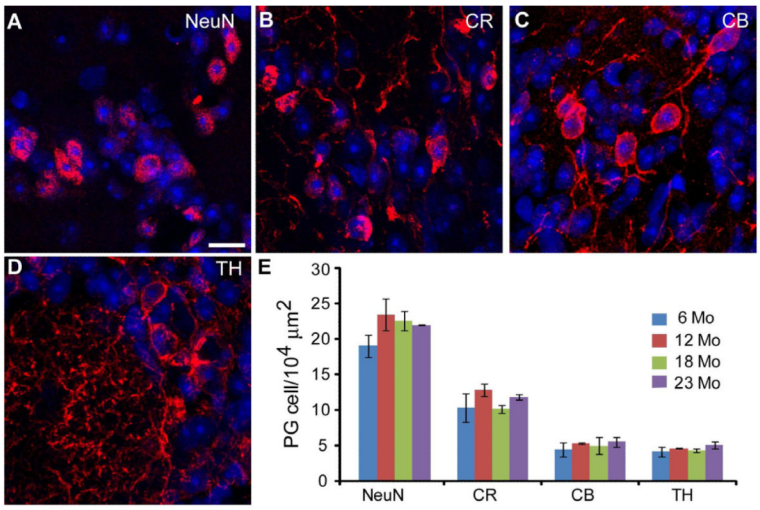

Figure 6.

PG cell populations are stable with aging. A-D, Subpopulations of PG cells in the GL of the OB stained for NeuN (A), calretinin (B), calbindin (C) and tyrosine hydroxylase (D). Scale bar = 10 μm. E, PG cell markers show no statistically significant changes in density with age.

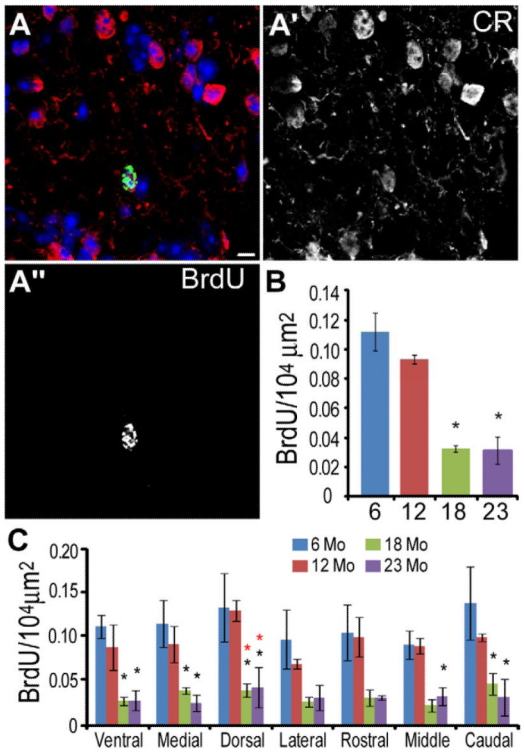

Figure 7.

The density of BrdU+ PG cells declines significantly with age in all regions of the GL. A, BrdU (green) colocalized with a calretinin+ (red) PG cell. A' calretinin. A" BrdU. Scale bar = 5 μm. B, Density of BrdU+ PG cells across ages (one-way ANOVA $p < 0.001$, Bonferroni posthoc test 6 and 12 mo vs 18 and 23 mo, $p < 0.01$, indicated by asterisk). C, Histogram showing BrdU+ cell density in each region of the OB for each age group. Each region significantly decreased with age (one-way ANOVA, $p < 0.05$; Bonferroni posthoc test, $p < 0.05$, asterisk indicates significant difference from 6 mo (black *) or 12 mo (red *) animals).